DOI: 10.1002/chem.201002748

From Helix to Macrocycle: Anion-Driven Conformation Control of π-Conjugated Acyclic Oligopyrroles

Yohei Haketa[a] and Hiromitsu Maeda*[a, b]

Abstract: Anion-responsive pyrrole-based linear receptor oligomers were newly synthesized and their anion-driven dynamic conformation changes were investigated. Phenylene-bridged dimers and a tetramer of dipyrrolyldiketone boron complexes as π-conjugated acyclic anion receptors formed anion-driven helical structures in the solid and solution states. In fact, single-crystal X-ray analyses of the receptor-anion complexes exhibited various helical structures, such as [1+1]- and [1+2]-type single helices and a [2+2]-type double helix according to the lengths of oligomers and the existence of terminal aryl substituents. Anion-binding modes and behaviors of the oligomers in solution state were also examined by ^{1}H NMR and UV/Vis spectra along with ESI-TOF MS. Differences in the binding modes were observed in the solid and solution states. The oligomers showed augmented anion-binding constants and anion-tunable electronic and optical properties in comparison with the monomer receptor. A negative cooperative effect in the tetramer was observed in the second anion binding of the [1+2]-type single helix due to electrostatic repulsion between two anions captured in the helix. Further, an anion-template coupling reaction from the linear dimer provided a receptor macrocycle, which was obtained as a Cl^- complex with distinct electronic and optical properties. The macrocycle exhibited extremely high anion-binding constants ($>10^{10}\,M^{-1}$ in CH_2Cl_2) through multiple hydrogen bonding.

Keywords: anions · heterocycles · host–guest systems · receptors · supramolecular chemistry

Introduction

The geometry of molecules, such as cyclic and linear structures, is an essential factor that determines their electronic and optical properties and preferred folding and assembling modes. In contrast to the fairly rigid cyclic geometries observed in hemes and cyclodextrins, linear oligomer and polymer structures in biotic systems can afford various spirals such as protein α-helices and DNA double helices.[1] Similar to biological systems, the guest-responsive regulation of helical structures that comprise synthetic molecules can be achieved by using noncovalent interactions such as hydrogen bonding and van der Waals forces.[2] In particular, π-conjugated oligomers with guest-binding abilities are fascinating components of such helical structures and are attractive because of their potential to show characteristic and tunable electronic states and form assemblies. Among the various "glues" available for folding helical structures together, positively charged species such as metal cations have been widely used thus far.[2a,3] Anions also play essential roles in the formation of complexes with organic receptor molecules through electrostatic hydrogen bonding, thereby yielding various assembled structures.[4] However, only a few anion-driven helical structures have been reported[5,6] because only few suitable motifs can form anion-responsive oligomer systems. Therefore, to fabricate such folding structures, it is necessary to design and synthesize appropriate anion-receptor molecules that exhibit high affinities for anions and can be transformed into oligomers.

As candidates for the building subunits, BF_2 complexes of 1,3-dipyrrolyl-1,3-propanediones (e.g., **1a**) exhibit anion-driven dynamic conformational changes such as the inversion of pyrrole rings (Scheme 1a).[7,8] Anion receptors, which allow absorption and emission in the visible region, can behave as sensors for anions and, thus, are potential elec-

[a] Y. Haketa, Prof. Dr. H. Maeda
College of Pharmaceutical Sciences
Institute of Science and Engineering, Ritsumeikan University
Kusatsu 525–8577 (Japan)
Fax: (+81) 77-561-2659
E-mail: maedahir@ph.ritsumei.ac.jp

[b] Prof. Dr. H. Maeda
PRESTO (Japan) Science and Technology Agency (JST)
Kawaguchi 332-0012 (Japan)

Supporting information for this article is available on the WWW under http://dx.doi.org/10.1002/chem.201002748.

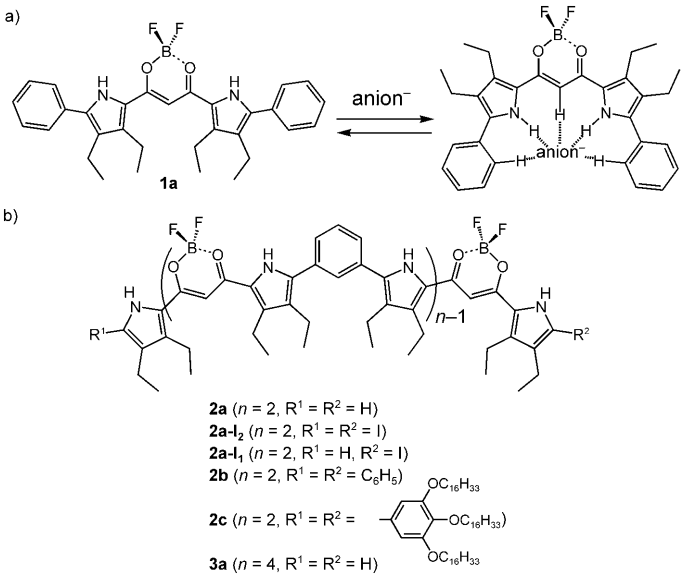

Scheme 1. a) Anion-binding mode and b) oligomeric derivatives of π-conjugated acyclic anion receptors.

tronic and optical materials. Thus, covalently linked oligomers (e.g., **2a**,[8c] Scheme 1b) exhibit folding behavior and resulting drastic changes in electronic and optical properties because of multiple hydrogen bonding with anions. Here we report the formation and properties of anion-responsive linear oligomers with various helical structures, along with a macrocycle as an extremely efficient anion-binding agent. In particular, linear oligomers are required to arrange their conformations by multiple inversions of π-conjugated moieties such as pyrrole rings. Stable orientations of pyrrole rings, the NH site of which faces toward oxygen in the absence of anions, induce anion-driven conformation changes. Fairly slow folding processes due to pyrrole inversions enable us to evaluate time-resolved spectral changes according to anion binding and to find that estimated kinetic parameters were correlated with the lengths of oligomers. To the best of our knowledge, this is the first report that discusses the kinetics of the formation of artificial helical structures.

Results and Discussion

Synthesis of anion receptor oligomers: The Suzuki coupling reaction of the bis-iodo-substituted dimer **2a-I$_2$**[8c] with phenylboronic acid gave terminal-α-aryl-substituted **2b** and **2c** in 48 and 18% yields, respectively. The same protocols can also be applied to the synthesis of higher oligomers such as tetramer **3a** from mono-iodo **2a-I$_1$** and 1,3-benzenediboronic acid bis(pinacol)ester in an 8% yield. UV/Vis absorption maxima (λ_{max}) of the oligomers in CH_2Cl_2 are 489 nm for **2a**,[8c] 514 nm for **2b**, and 478 nm for **3a**, thus suggesting no significant π extension relative to monomer **1a** (499 nm)[8c] due to the cross-conjugated *meta*-phenylene spacer(s) along with the distortion of planarity. In particular, the broad absorption band of **3a** with a shoulder at 515 nm suggests the formation of partially folding structures. From the UV/Vis spectra, which show almost no or weak exciton couplings of the receptor units, the oligomers basically prefer linear conformations in the absence of anions. Further, fluorescence emissions of **2a**,**b** and **3a** were observed at 511, 545, and 564 nm with quantum yields (Φ_F) of 0.89, 0.91, and 0.73, respectively.

Solid-state anion-binding behaviors of linear oligomers: The formation of anion-driven helical structures was initially elucidated by the single-crystal X-ray analysis of anion complexes of receptor oligomers prepared by treatment with a tetrapropylammonium (TPA) salt of Cl^- (Figure 1). In the solid state, driven by Cl^- complexation, **2a** and **3a** form single helices, whereas **2b** forms a double helical structure. All the crystals are racemic states containing equimolar *M* and *P* helices. In **2a**·Cl^-, which forms a [1+1]-type helix, pyrrole rings are completely inverted to bind Cl^- through multiple hydrogen bonding. In this case, the terminal α-CH moieties with distances of 3.510(9) and 3.629(8) Å are slightly overlapped to construct a single helix. Two of either *M* or *P* strands of **2a** are stacked at distances of 3.4–3.5 Å to form

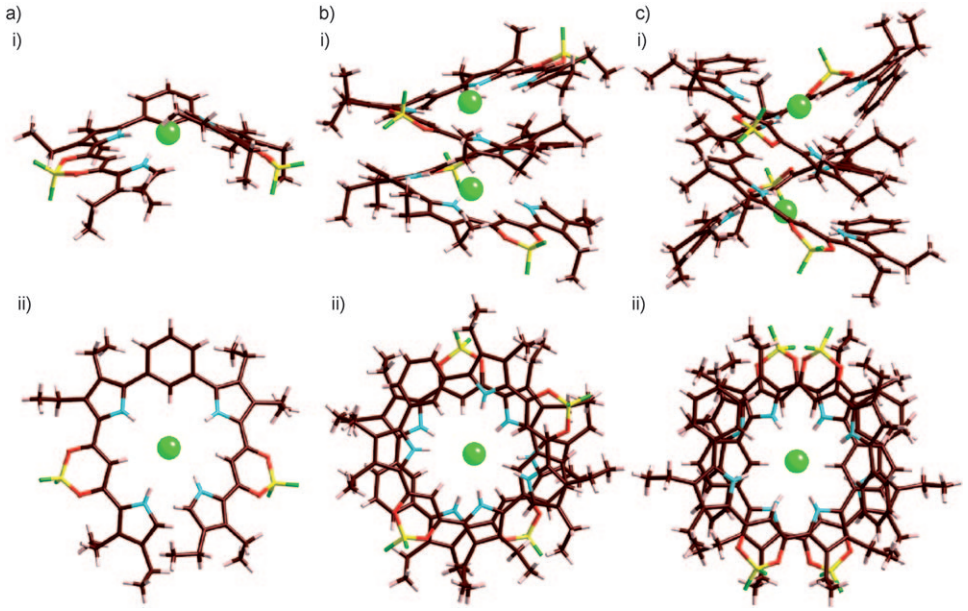

Figure 1. Single-crystal X-ray structures in i) side and ii) top view) as *M* helices of a) **2a**·Cl^- (one of the two independent structures), b) **3a**·Cl^-_2 (one of the two independent structures), and c) **2b$_2$**·Cl^-_2. Solvents and TPA cations are omitted for clarity. Atom color code: brown, pink, yellow, green, blue, and red refer to carbon, hydrogen, boron, fluorine, nitrogen, and oxygen, respectively.

dimers and their piled-up structures with TPA cations. In contrast, for **3a**·Cl^-_2, intramolecular π–π stacking of the tetramer assisted by two Cl^- is crucial for the formation of the [1+2]-type single helix. The distance between two Cl^- is 4.638(2)/4.632(2) Å, and each Cl^- is bound by half of the tetramer. Single helices of **3a** are also piled up to form the columnar structures that consist of either enantiomer. In sharp contrast to **2a** and **3a**, which form single helices, α-phenyl-substituted dimer **2b** exhibits the formation of [2+2]-type assemblies, in which two strands bind two Cl^- by six hydrogen bonds for each anion: hydrogen-bonding distances to Cl^- in **2b**$_2$·Cl^-_2 are 3.551(2) and 3.552(2) Å by outer NH, 3.279(2) and 3.270(2) Å by inner NH, and 3.410(2) and 3.424(2) Å by bridging CH for each anion.[9] Two Cl^- are located with the distance of 5.802(14) Å inside the channel structure, which is capped by TPA cations. Although *o*-CH sites of the terminal phenyl rings and center phenylene–CH show no significant interactions with anions, π–π stacking between two strands stabilizes the double helices; the distance between two helical planes of **2b** is in the range of 3.4–3.5 Å. Layers that comprise double helices with the same chirality are alternatively stacked with other layers that have counter chirality.

Anion-binding behaviors of linear oligomers in solution state: Formation of [1+1]-type single helices of **2a**,**b** in the solution state, which were also supported by other methods discussed later, was initially examined by means of NMR spectral changes. For example, upon the addition of 1.0 equiv of Cl^- as a tetrabutylammonium (TBA) salt to a solution of **2b** in CD_2Cl_2 at 20 °C, ^{1}H NMR spectroscopic signals at $\delta = 9.49$ (NH^a), 9.43 (NH^b), 7.69 (CH^d), and 6.60 ppm (CH^e) decreased in intensity with the concurrent appearance of new signals (and shifted values) at $\delta = 11.32$ (+1.83), 10.32 (+0.89), 8.65 (+0.96), and 7.75 ppm (+1.15), respectively (Figure 2a, i), thereby suggesting the formation of a Cl^- complex. In particular, the difference between NH^a and NH^b ($\delta = 1.00$ ppm) indicates the existence of [1+1]-type helices, not [2+2]-type, in the solution state because of the weak interaction by NH^b due to the existence of the

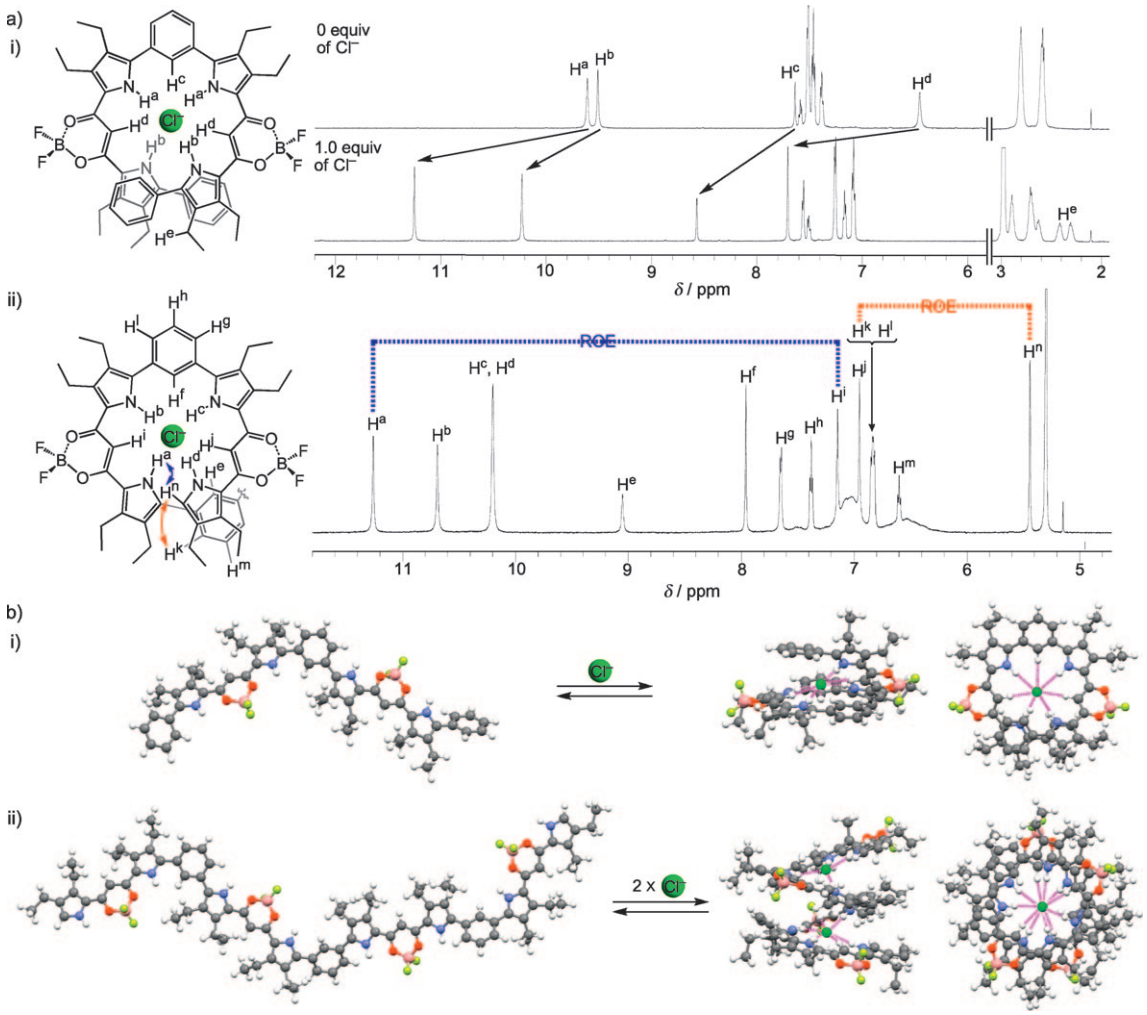

Figure 2. a) Schematic representations of Cl^- complexes (left) and ^{1}H NMR spectral changes in CD_2Cl_2 upon the addition of TBACl (1 and 2 equiv, respectively; right) of i) **2b** and ii) **3a** (ROE correlations are indicated). b) DFT-optimized structures of i) **2b** and **2b**·Cl^- (side and top view) and ii) **3a** and **3a**·Cl^-_2 (side and top view).

neighboring terminal phenyl moiety. In addition, there are no driving forces to assemble two [1+1]-type single helices to double helices in the solution state. At −50 °C, the ^{1}H NMR spectroscopic signal of β-ethyl-CH_2 units (e.g., H^e) of **2b**·Cl^- splits into two complicated signals through diastereotopic coupling due to the formation of helical structures. Similarly, the ^{19}F NMR spectroscopic signal for the BF_2 moiety of **2b** at −50 °C exhibited a singlet peak at $\delta = -142.2$ ppm and split into two doublet signals at $\delta = -142.1$ and −143.6 ppm with ^{19}F,^{19}F coupling constants of 82 Hz upon the addition of 1.0 equiv of Cl^-. At 20 °C, only broad and coalesced signals were observed, which may be due to the faster interconversion between helical enantiomers. On the other hand, **2a**·Cl^- showed weak diastereotopic coupling in ^{1}H and ^{19}F NMR spectra even at −90 °C because of the absence of terminal aryl rings, and the [1+1]-type Cl^- complex of **2c** exhibited split ^{19}F NMR spectroscopic signals even at RT due to slower interconversion. Dimers **2a–c**, even with an excess amount of Cl^- (10 equiv), showed [1+1] binding to be the most stable mode.[10]

In the presence of 2 equiv of TBACl in CD_2Cl_2 at −50 °C, tetramer **3a**, which is less soluble without TBA salts of anions in this solvent, showed downfield ^{1}H NMR spectroscopic signals at $\delta = 11.30$ (NH^a), 10.75 (NH^b), 10.28 ($NH^{c,d}$), 9.09 (CH^e), 8.02 (CH^f), 7.21 (CH^i), and 7.01 ppm (CH^j) that were ascribable to the interaction sites of **3a**·Cl^-_2. Due to the low solubility of **3a**, the details of the [1+1]-type complex could not be examined at the millimolar-order concentration in CD_2Cl_2. The helical structure of **3a**·Cl^-_2 as observed in the solid state was suggested by the downfield shift of CH^e interacting with both Cl^-; this was also supported by COSY and ROESY, particularly the correlations between CH^n and NH^a and between CH^n and CH^k (Figure 2a, ii). Terminal α-CH^n was observed at $\delta = 5.49$ ppm, which is upfield shifted at $\delta = 0.71$ ppm compared to the corresponding CH of **2a**·Cl^-; this is presumably due to the shielding effect of the stacking pyrrole unit. Four sets of signals in the ^{19}F NMR spectra also suggested a helical structure. Other possible binding modes, including an unfolded [1+4] complex, were not observed in the presence of an excess amount (10 equiv) of TBACl under these conditions. Anion-binding single helices of **2a**·Cl^-, **2b**·Cl^-, and **3a**·Cl^-_2 in the solution state are also supported by the theoretically optimized structures (Figure 2b, right),[11,12] which are completely different conformations of the optimized conformations of the anion-free oligomers (Figure 2b, left).

Characteristic points of the pyrrole-based oligomers **2a–c** and **3a** are electronic and optical properties that can be tuned by anion binding and the resulting molecular folding. The oligomers showed dramatic anion-driven changes in the UV/Vis absorption and fluorescence spectra. Upon the addition of Cl^- as a TBA salt, the absorption bands of **2a–c** at 489, 514, and 521 nm in CH_2Cl_2 decreased with new bands at 444, 474, and 484 nm, respectively, presumably due to the exciton coupling of the monomeric chromophore units (Figure 3a). Tetramer **3a** exhibited the stepwise spectral changes for [1+1]- and [1+2]-type binding under diluted conditions.

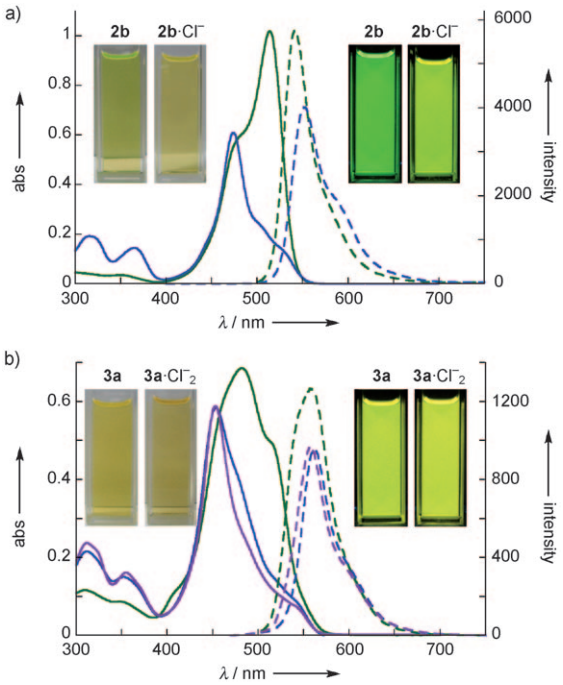

Figure 3. UV/Vis (solid line) and fluorescence (broken line, excited at a) 478 and b) 458 nm) spectra: a) **2b** (green), **2b**·Cl^- (blue), and photographs of **2b** and **2b**·Cl^- (inset) in CH_2Cl_2 (5 μM); b) **3a** (green), **3a**·Cl^- (blue), and **3a**·Cl^-_2 (purple), and photographs of **3a** and **3a**·Cl^-_2 (inset) in CH_2Cl_2 (2.5 μM).

This resulted in a shift of the absorption at 476 nm in CH_2Cl_2 to those at 452 and 453 nm that corresponded to **3a**·Cl^- and **3a**·Cl^-_2, respectively, by the addition of 2 and 2000 equiv of Cl^- (Figure 3b). On the other hand, under the same conditions, fluorescence emissions of **2a**,**b** and **3a** changed to those observed at 520, 550, and 562/556 nm with quantum yields (Φ_F) of 0.72, 0.76, and 0.50/0.48, respectively. The anion-binding modes were supported by Job plots (**2b**), stepwise spectral changes (**3a**), and ESI-TOF MS of Cl^- complexes of the oligomers: [1+1]-type complexes for **2a**,**b** and a [1+2]-type complex for **3a** in the solution state. In the case of **2b**, the binding mode in solution is different from that in the solid state, which may induce further aggregation of the [1+1] complex to afford a [2+2]-type double helix. To the best of our knowledge, **3a**·Cl^-_2 is the first example of a single helix that contains two anions,[13] the electrostatic repulsion of which may be subdued by other factors, such as the formation of stable folding structure. Further, **2a–c** and **3a** exhibited significantly augmented binding constants K_a for halide anions in CH_2Cl_2, determined by UV/Vis absorption spectral changes upon the addition of TBA salts (Table 1). For example, K_a values in the [1+1] complexation with Cl^- are 5.9×10^7, 1.2×10^7, and $1.2\times10^8\,M^{-1}$, respectively, which are much higher than that of **1a** ($2700\,M^{-1}$). The K_a values for Br^- and I^- in CH_2Cl_2 were 4.8×10^6 and $5.8\times10^4\,M^{-1}$ for **2a**, 2.4×10^4 and $6.8\times10^3\,M^{-1}$ for **2b**, 2.3×10^7 and $8.8\times10^4\,M^{-1}$ for **3a**, and 300 and $14\,M^{-1}$ for **1a**, respectively. These oligomers show the selectivity for halide anions as $Cl^- > Br^- > I^-$ according to their basicities and ion sizes. Fur-

Table 1. Binding constants (K_a, M^{-1}) of **1a** (reference), **2a–c**, and **3a** with various halide anions in CH_2Cl_2.[a]

	1a[b]	**2a**	**2b**	**2c**		**3a**
Cl^-	2700	59000000	12000000	850000	K_1:	120000000
					K_2:	3200
Br^-	300	4800000	24000	38000	K_1:	23000000
					K_2:	1600
I^-	17	58000	6800	130	K_1:	88000
					K_2:	33

[a] The errors in K_a for anions are within 10% as observed in the Supporting Information. [b] Ref. [8c].

ther, K_2 values of **3a** for Cl^-, Br^-, and I^- are 3200, 1600, and 33 M^{-1}, respectively, which are smaller than those of [1+1]-type binding.[14] This result suggests the significant negative cooperativity of **3a** for second anion binding presumably due to electronic repulsions between two anions captured in the helices.

UV/Vis absorption spectral changes of **2a–c** and **3a** as detected by stopped-flow measurements (Figure 4) exhibited the time-resolved anion-driven dynamic conformation changes and kinetic parameters k of **2a–c** and **3a** as 1.2×10^7, 4.8×10^6, 1.6×10^6, and $1.2\times10^6\,M^{-1}s^{-1}$, respectively, for [1+1] complexation with Cl^-. This result suggests a slower folding process by longer oligomers even when possessing higher anion affinities. The examination here is the first example of the time-resolved detection of the formation of ordered synthetic helical structures. The timescale detectable

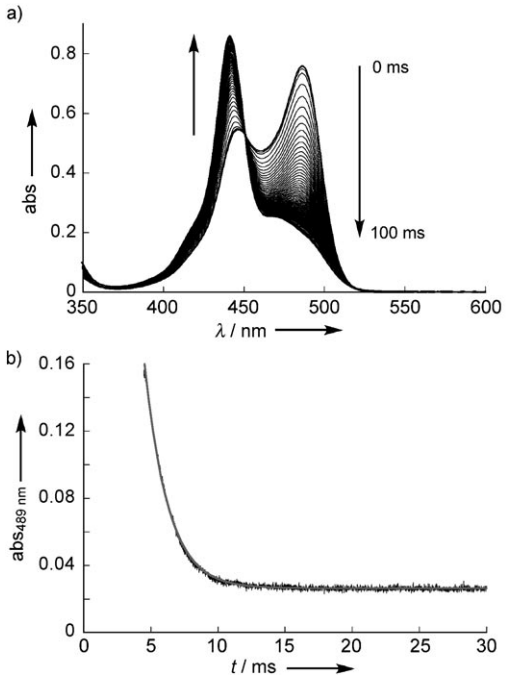

Figure 4. a) Time-resolved UV/Vis absorption spectral changes and b) time-dependent changes at 489 nm detected by stopped-flow measurement of **2a** (5 μM) upon the addition of Cl^- (1 and 10 equiv for i and ii, respectively) as a TBA salt in CH_2Cl_2. Different time scales in i and ii depend on the amounts of added anion: detailed time-resolved examination in ii requires an excess amount of anion due to the analysis through pseudo-first-order kinetic parameters.

by stopped-flow measurements has been correlated with the conformation changes, which require the inversions of pyrrole rings. Furthermore, fairly flexible behaviors in the helical Cl^- complexes of the oligomers were also suggested by variable-temperature absorption spectra.

Synthesis and properties of the macrocycle that exhibits extremely high anion affinity: The crystal and optimized structures of **2a**·Cl^- inspired us to connect the proximal terminal pyrrole α-positions of **2a** to obtain cyclic structures. The Pd-catalyzed intramolecular coupling[15] of **2a-I$_2$** provided macrocycle **4a** in a 31% yield with the existence of Cl^- (TBACl) as a template. To our surprise, **4a** was isolated as a TBA salt of a stable Cl^- complex (**4a**·Cl^-; Figure 5a, i) even after purification by several executions of silica gel column chromatography. The ^1H NMR spectra of **4a**·Cl^- in CD_2Cl_2 at 20 °C showed signals at $\delta=11.74$ (NH^a), 10.83 (NH^b), 8.72 (CH^c), and 8.39 ppm (CH^d) (Figure 5a, ii), which shifted downfield relative to the corresponding protons of **2a**. At −50 °C, new signals corresponding to twisted sandwichlike dimer **4a**$_2$·Cl^- appear at 10.13, 9.34, 9.27, and 8.86 ppm for NH, and $\delta=7.75$, 7.50, 7.45, 7.30, 7.04, 6.81, and 6.58 ppm for other protons. The dimerization constant K_{dim}, defined as $([\mathbf{4a}_2\cdot Cl^-][Cl^-])/[\mathbf{4a}\cdot Cl^-]^2$, is estimated to be 2.5×10^{-3} at −50 °C. By the addition of another 1 equiv of TBACl, the stacking dimer cannot be observed.[16] In addition, the removal of Cl^- in **4a**·Cl^- was attempted by treatment with various Ag^+ salts; it resulted in the formation of a complicated mixture including decomposed species. On the basis of these observations, Cl^- was found to be tightly bound by **4a** and to stabilize this cyclic structure; competitive titration of **2a** with **4a**·Cl^- suggested an extremely high K_a value of **4a** for Cl^- (ca. $2\times10^{10}\,M^{-1}$) in CH_2Cl_2. This value is much higher than that of the triazole-based macrocycle, $1.1\times10^7\,M^{-1}$ in CH_2Cl_2.[5e,17] Further, relative to acyclic **2a** and **2a**·Cl^-, cyclic **4a**·Cl^- in CH_2Cl_2 exhibited unique electronic properties in a fairly sharp absorption band at 450 nm along with a broad band around 605 nm (Figure 5b, i). Interestingly, in contrast to **2a** and **2a**·Cl^-, the macrocycle **4a**·Cl^- showed a redshifted emission at 660 nm ($\lambda_{ex}=450$ nm) with Φ_F of 0.31 in CH_2Cl_2 (Figure 5b, ii).

Conclusion

The linear and cyclic structures reported here are fascinating molecular architectures and potential building blocks of stimuli-responsive utility materials. Compared to anion-assisted helical structures reported thus far, the electronic and optical properties of the oligopyrrole systems reported here can be controlled by anions, because the flexibility, stability, and π conjugation of these oligomers are suitable for visible light excitation and direct electronic perturbation in pyrrole NH by anion binding. Significant changes in conformations by anions are due to the requirement of inversions of pyrrole rings that result in the formation of helical structures. Time-resolved observations of the changes in the electronic

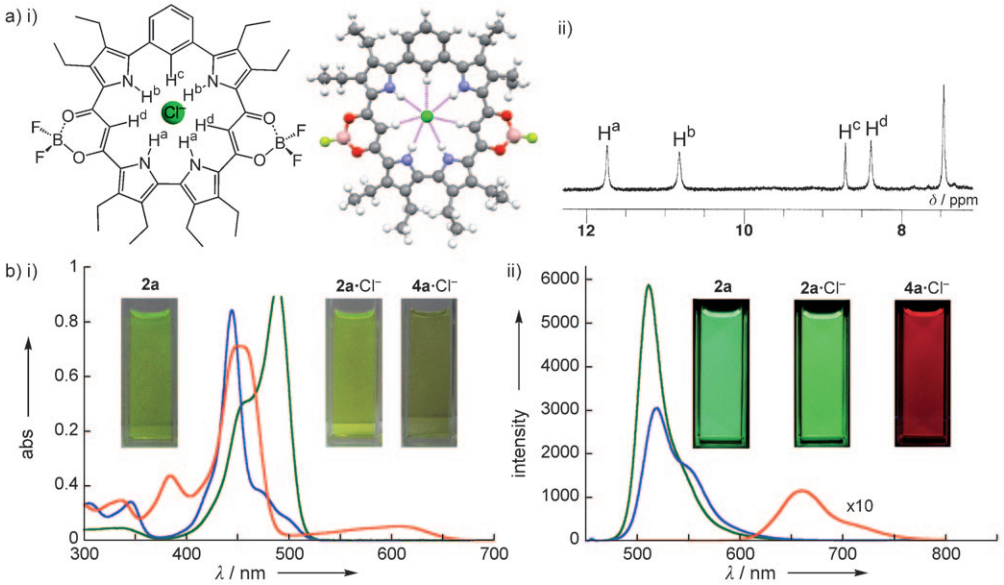

Figure 5. a) i) Schematic and DFT-optimized structure of **4a**·Cl^- and ii) selected ^1H NMR spectrum of **4a**·Cl^- as a TBA salt in CD_2Cl_2 (1 mM) at RT; b) i) UV/Vis and ii) fluorescence spectra (excited at 453 nm for **2a** and **2a**·Cl^- and 450 nm (λ_{max}) for **4a**·Cl^-) of **2a** (green), **2a** plus 1 equiv of Cl^- (blue), and **4a**·Cl^- (red) in CH_2Cl_2 (5 μM for **2a** and **2a**·Cl^-, 10 μM for **4a**·Cl^-) and their photographs (inset).

states by anion binding revealed the effects of lengths of the oligomers for folding behaviors. Further higher organization of helical and cyclic structures assisted by peripheral modification, along with chiral amplification in helices induced by appropriate chiral auxiliaries, would help in the realization of utility devices such as circular polarized light emitters in the near future.

Experimental Section

General procedures: Starting materials were purchased from Wako Pure Chemical Industries Ltd., Nacalai Tesque Inc, and Sigma–Aldrich Co. and used without further purification unless otherwise stated. UV-visible spectra were recorded using a Hitachi U-3500 spectrometer. Fluorescence spectra were recorded using a Hitachi F-4500 fluorescence spectrometer for ordinary solutions and a Hamamatsu Quantum Yields Measurements System for Organic LED Materials C9920-02 for measurement of quantum yields. NMR spectra used in the characterization of products were recorded using a JEOL ECA-600 600 MHz spectrometer. All NMR spectra were referenced to solvent. Matrix-assisted laser desorption ionization time-of-flight mass spectrometries (MALDI-TOF MS) were recorded using a Shimadzu Axima-CFRplus in negative mode. Electrospray ionization mass spectrometric studies (ESI-MS) were recorded using a Bruker microTOF with the negative mode ESI-TOF method. TLC analyses were carried out on aluminum sheets coated with silica gel 60 (Merck 5554). Column chromatography was performed using Sumitomo alumina KCG-1525, Wakogel C-200, C-300, and Merck silica gel 60 and 60H.

Diphenyl-substituted phenylene-bridged dimer (2b): A Schlenk tube filled with **2a-I$_2$**[8c] (62.1 mg, 0.059 mmol), phenylboronic acid (15.83 mg, 0.129 mmol), tetrakis(triphenylphosphine)palladium(0) (11.56 mg, 0.01 mmol), and cesium carbonate (67.67 mg, 0.18 mmol) was flushed with nitrogen and charged with a mixture of degassed DMF (3 mL), toluene (3 mL), and water (0.1 mL). The mixture was heated at 90 °C for 20 h, cooled, then partitioned between water and CH_2Cl_2. The combined extracts were dried over anhydrous $MgSO_4$ and evaporated. The residue was then chromatographed over silica gel flash column (eluent: 1% MeOH/CH_2Cl_2) and recrystallized from CH_2Cl_2/hexane to give **2b** (17.3 mg, 48%) as a red solid. R_f=0.30 (1% MeOH/CH_2Cl_2); ^1H NMR (600 MHz, $CDCl_3$, 20 °C): δ=9.38 (s, 2H; NH), 9.35 (s, 2H; NH), 7.65 (s, 1H; phenylene-CH), 7.62–7.60 (m, 1H; phenylene-CH), 7.55–7.54 (m, 2H; phenylene-CH), 7.53–7.52 (m, 4H; phenyl-*o*-CH), 7.50–7.47 (m, 4H; phenyl-*m*-CH), 7.43–7.40 (m, 2H; phenyl-*p*-CH), 6.59 (s, 2H; bridged-CH), 2.88 (m, 8H; CH_2CH_3), 2.65 (m, 8H; CH_2CH_3), 1.38–1.35 (m, 12H; CH_2CH_3), 1.23–1.19 ppm (m, 12H; CH_2CH_3); UV/Vis (CH_2Cl_2): λ_{max} (ε)=514.0 nm (2.4×10^5 M^{-1}cm^{-1}); fluorescence (CH_2Cl_2): λ_{em} (λ_{ex})= 546.0 nm (514.0 nm); ESI-TOF MS: *m*/*z*: (%): 949.46 (100), 950.47 (56); calcd for $C_{56}H_{59}B_2F_4N_4O_4$: 949.47 $[M-H]^-$. This compound as a Cl^- complex was further characterized by X-ray diffraction analysis.

Bis(3,4,5-trihexadecyloxyphenyl)-substituted phenylene-bridged dimer (2c): A Schlenk tube filled with **2a-I$_2$**[8c] (80.0 mg, 0.076 mmol), 3,4,5-trihexadecyloxyphenylboronic acid pinacol ester[8g] (176.2 mg, 0.19 mmol), tetrakis(triphenylphosphine)palladium(0) (21.96 mg, 0.019 mmol), and cesium carbonate (185.7 mg, 0.57 mmol) was flushed with nitrogen and charged with a mixture of degassed DMF (2.5 mL), toluene (2.5 mL), and water (0.2 mL). The mixture was heated at 90 °C for 20 h, cooled, then partitioned between water and CH_2Cl_2. The combined extracts were dried over anhydrous $MgSO_4$ and evaporated. The residue was then chromatographed over silica gel flash column (eluent: 0.5% MeOH/CH_2Cl_2) and recrystallized from CH_2Cl_2/MeOH to give **2c** (33.3 mg, 18%) as a red solid. R_f=0.30 (1% MeOH/CH_2Cl_2); ^1H NMR (600 MHz, $CDCl_3$, 20 °C): δ=9.37 (s, 2H; NH), 9.28 (s, 2H; NH), 7.64 (s, 1H; phenylene-CH), 7.62–7.59 (m, 1H; phenylene-CH), 7.55–7.53 (m, 2H; phenylene-CH), 6.66 (s, 4H; phenyl-*o*-CH), 6.57 (s, 2H; bridged-CH), 4.02–4.00 (m, 12H; OCH_2), 2.88–2.84 (m, 8H; CH_2CH_3), 2.66 (q, J=7.8 Hz, 4H; CH_2CH_3), 2.62 (q, J=7.8 Hz, 4H; CH_2CH_3), 1,83 (tt, J=7.2 and 6.6 Hz, 8H; OCH_2CH_2), 1.77 (tt, J=7.2 and 6.6 Hz, 4H; OCH_2CH_2), 1.52–1.47 (m, 12H; $OC_2H_4CH_2$), 1.37–1.34 (m, 12H; CH_2CH_3), 1.34–1.25 (m, 144H; $OC_3H_6C_{12}H_{24}$), 1.22–1.19 (m, 12H; CH_2CH_3), 0.88–0.86 ppm (m, 18H; $OC_{15}H_{30}CH_3$); UV/Vis (CH_2Cl_2): λ_{max} (ε)=521.5 nm (2.2×10^5 M^{-1}cm^{-1}); fluorescence (CH_2Cl_2): λ_{em} (λ_{ex})=557.0 (521.0 nm); ESI-TOF MS: *m*/*z* (%): 2390.94 (100), 2391.95 (73); calcd for $C_{152}H_{251}B_2F_4N_4O_{10}$: 2390.94 $[M-H]^-$.

Tetramer (3a): A Schlenk tube filled with **2a-I$_1$**[8c] (230.0 mg, 0.249 mmol), benzene-1,3-diboronic acid pinacol ester (41.09 mg, 0.124 mmol), tetrakis-(triphenylphosphine)palladium(0) (28.89 mg, 0.025 mmol), and cesium carbonate (121.21 mg, 0.372 mmol) was flushed with nitrogen and charged with a mixture of degassed DMF (4 mL), toluene (4 mL), and water (0.1 mL). The mixture was heated at 90 °C for

20 h, cooled, then partitioned between water and CH_2Cl_2. The combined extracts were dried over anhydrous $MgSO_4$ and evaporated. The residue was then chromatographed over silica gel flash column (eluent: 1% MeOH/$CHCl_3$) to give **3a** (12.4 mg, 6%) as a red solid. $R_f = 0.44$ (3% MeOH/$CHCl_3$); ^{1}H NMR (600 MHz, [D_8]THF, 20°C: [D_8]THF was used due to the low solubility of **3a** in $CDCl_3$ in the absence of anions as TBA salts): $\delta = 11.42$ (s, 2H; NH), 11.34 (s, 6H; NH), 7.78 (s, 3H; phenylene-CH), 7.60 (m, 6H; phenylene-CH), 7.57 (m, 3H; phenylene-CH), 7.02 (s, 2H; pyrrole-CH), 6.63 (s, 2H; bridged-CH), 6.54 (s, 2H; bridged-CH), 2.94 (m, 12H; CH_2CH_3), 2.85 (m, 4H; CH_2CH_3), 2.67 (m, 12H; CH_2CH_3), 2.51 (m, 4H; CH_2CH_3), 1.36 (m, 18H; CH_2CH_3), 1.28 (m, 6H; CH_2CH_3), 1.22 (m, 6H; CH_2CH_3), 1.18 ppm (m, 18H; CH_2CH_3); UV/Vis (CH_2Cl_2): λ_{max} (ε) = 478.0 nm ($2.8\times10^5\,M^{-1}cm^{-1}$); The ε value in CH_2Cl_2 was estimated by means of a soluble THF stock solution, the concentration of which was determined by integrals of ^{1}H NMR spectroscopy in [D_8]THF in comparison with a reference additive (EtOAc in this case); fluorescence (CH_2Cl_2): λ_{em} (λ_{ex}) = 564.0 nm (478.0 nm); ESI-TOF MS: *m/z* (%): 1669.82 (100); calcd for $C_{94}H_{105}B_4F_8N_8O_8$: 1669.84 $[M-H]^-$. This compound as a Cl^- complex was further characterized by X-ray diffraction analysis.

Macrocycle as a TBACl complex (4a·TBACl): A Schlenk tube filled with **2a-I$_2$**[8c] (170.0 mg, 0.162 mmol), hydroquinone (93.67 mg, 0.85 mmol), cesium carbonate (554.2 mg, 1.70 mmol), and tetrabutylammonium chloride (907.14 mg, 3.26 mmol) was degassed and flushed with nitrogen, and charged with degassed DMA (68 mL). Then the solution of palladium acetate (19.04 mg, 0.085 mmol) and tri(*o*-tolyl)phosphine (25.84 mg, 0.085 mmol) in degassed DMA (5 mL) was added. The mixture was heated at 95°C for 2 d, cooled, then partitioned between water and CH_2Cl_2. The combined extracts were dried over anhydrous $MgSO_4$ and evaporated. The residue was then chromatographed over silica gel flash column (eluent: 3% MeOH/CH_2Cl_2 and 40% EtOAc/hexane) and recrystallized from CH_2Cl_2/hexane to give **4a**·TBACl (53.6 mg, 31%) as a dark green solid. ^{1}H NMR (600 MHz, $CDCl_3$, 20°C): $\delta = 11.63$ (s, 2H; NH), 10.73 (s, 2H; NH), 8.70 (s, 1H; phenylene-CH), 8.36 (s, 2H; bridged-CH), 7.43 (m, 3H; phenylene-CH), 2.94 (t, $J = 8.4$ Hz, 8H; NCH_2), 2.88 (m, 8H; CH_2CH_3), 2.68 (m, 4H; CH_2CH_3), 2.59 (q, $J = 7.2$ Hz, 4H; CH_2CH_3), 1.41 (m, 8H; NCH_2CH_2), 1.24 (m, 18H; CH_2CH_3), 1.14 (m, 6H; CH_2CH_3), 1.14 (m, 8H; $NC_2H_4CH_2$), 0.81 ppm (t, $J = 7.2$ Hz, 12H; $NC_3H_6CH_3$); UV/Vis (CH_2Cl_2): λ_{max} (ε) = 450.0 nm ($1.0\times10^5\,M^{-1}cm^{-1}$); fluorescence ($CH_2Cl_2$): λ_{em} (λ_{ex}) = 660.0 nm (450.0 nm); ESI-TOF-MS: *m/z* (%): 831.34 (100); calcd for $C_{44}H_{50}B_2F_4N_4O_4Cl$: 831.37 $[M+Cl]^-$.

Single-crystal X-ray analysis: Crystallographic data for Cl^- complexes of receptor oligomers are summarized in Table 2. A single crystal of **2a**·TPACl was obtained by vapor diffusion of hexane into a 1,2-dichloroethane (10% toluene) solution. The data crystal was a yellow prism of approximate dimensions 0.50 mm × 0.20 mm × 0.10 mm. Data were collected at 90 K using a Bruker SMART CCDC diffractometer with graphite-monochromated $Mo_{K\alpha}$ radiation ($\lambda = 0.71075$ Å), and the structure was solved by direct methods. A single crystal of **2b$_2$**·$(TPACl)_2$ was obtained by vapor diffusion of hexane into a 1,2-dichloroethane solution. The data crystal was a red prism of approximate dimensions 0.40 mm × 0.30 mm × 0.20 mm. Data were collected at 123 K using a Rigaku RAXIS-RAPID diffractometer with graphite-monochromated $Mo_{K\alpha}$ radiation ($\lambda = 0.71075$ Å), and the structure was solved by direct methods. A single crystal of **3a**·$(TPACl)_2$ was obtained by vapor diffusion of octane into a 1,2-dichloroethane solution. The data crystal was an orange prism of approximate dimensions 0.40 mm × 0.30 mm × 0.20 mm. Data were collected at 123 K using a Rigaku RAXIS-RAPID diffractometer with graphite-monochromated $Mo_{K\alpha}$ radiation ($\lambda = 0.71075$ Å), and the structure was solved by direct methods. In each compound, the non-hydrogen atoms were refined anisotropically. The calculations were performed using the Crystal Structure crystallographic software package by the Molecular Structure Corporation.[18] The scattering that arose from the presence of disordered solvents in the crystals was removed by use of the utility SQUEEZE in the PLATON software package.[19,20] CCDC-778926 (**2a**·TPACl), 778927 (**2b$_2$**·$(TPACl)_2$), and 778928 (**3a**·$(TPACl)_2$) contain the supplementary crystallographic data for this paper. These data can be obtained free of charge from The Cambridge Crystallographic Data Centre via www.ccdc.cam.ac.uk/data_request/cif.

Table 2. Crystallographic details for anion complexes.

	2a·TPACl	**2b$_2$**·$(TPACl)_2$	**3a**·$(TPACl)_2$
formula	$C_{44}H_{52}B_2F_4N_4O_4$· TPACl·1.75 CH_2ClCH_2Cl	$C_{56}H_{60}B_2F_4N_2O_4$· TPACl·0.5 CH_2Cl_2	$C_{94}H_{106}B_4F_8N_8O_8$· $(TPACl)_2$
M_r	1193.49	1214.97	2114.72
crystal size [mm]	0.50 × 0.20 × 0.10	0.40 × 0.30 × 0.20	0.30 × 0.30 × 0.10
crystal system	monoclinic	monoclinic	triclinic
space group	$P2_1/c$ (no. 14)	$P2/c$ (no. 13)	$P\bar{1}$ (no. 2)
a [Å]	17.3673(12)	15.683(4)	19.305(3)
b [Å]	23.9699(16)	17.188(3)	24.644(3)
c [Å]	36.2984(19)	28.437(4)	29.522(5)
α [°]	90	90	88.52(5)
β [°]	118.387(3)	119.134(8)	81.42(6)
γ [°]	90	90	89.69(5)
V [Å^3]	13293.8(15)	6696(9)	13883(4)
ρ_{calcd} [g cm^{-3}]	1.193	1.205	1.012
Z	4	2	4
T [K]	90(2)	123(2)	123(2)
$\mu(Mo_{K\alpha})$ [mm^{-1}]	0.255	0.158	0.107
reflns	71657	57080	86346
unique reflns	24718	13719	38845
variables	1448	796	2748
$\lambda_{Mo_{K\alpha}}$ [Å]	0.71073	0.71069	0.71075
R_1 ($I > 2\sigma(I)$)	0.1078	0.0634	0.1112
wR_2 ($I > 2\sigma(I)$)	0.3071	0.1574	0.2689
GOF	1.025	1.037	0.914

Stopped-flow measurements: Stopped-flow measurements were carried out using a Unisoku RSP-1000 stopped-flow rapid-scan spectroscopy system.

DFT calculations: Ab initio and semiempirical calculations of linear and cyclic oligomers and their Cl^--binding complexes were carried out by using the Gaussian 03 program[11] and an HP Compaq DC5100 SFF computer. The structures were optimized, and the total electronic energies were calculated at the B3LYP level by using the 6-31G(d,p) and 6-31+G(d,p) basis sets and the AM1 level for oligomers and anion complexes.

Acknowledgements

This work was supported by a grant-in-aid for Young Scientists (B) (no. 21750155) and for Scientific Research in Priority Area "Super-Hierarchical Structures" (no. 19022036) from the MEXT and Ritsumeikan R-GIRO project (2008–2013). The authors thank Prof. Atsuhiro Osuka, Dr. Naoki Aratani, Dr. Yasuhide Inokuma, Mr. Eiji Tsurumaki, and Mr. Taro Koide, Kyoto University, for the X-ray analyses; Prof. Hiroshi Shinokubo and Dr. Satoru Hiroto, Nagoya University, for ESI-TOF MS measurements; and Prof. Hitoshi Tamiaki, Ritsumeikan University, for various measurements. Y.H. thanks JSPS for a Research Fellowship for Young Scientists.

[1] D. Voet, J. G. Voet, *Biochemistry*, 3rd ed., Wiley, New York, **2004**.
[2] Selected book and reviews for artificial helical structures: a) *Foldamers: Structures, Properties, and Applications* (Eds.: S. Hecht, I.

Huc), Wiley-VCH, Weinheim, **2007**; b) D. J. Hill, M. J. Mio, R. B. Prince, T. S. Hughes, J. S. Moore, *Chem. Rev.* **2001**, *101*, 3893–4011; c) E. Yashima, K. Maeda, Y. Furusho, *Acc. Chem. Res.* **2008**, *41*, 1166–1180; d) D. Haldar, C. Schmuck, *Chem. Soc. Rev.* **2009**, *38*, 363–371; e) H. Juwarker, J.-m. Suk, K.-S. Jeong, *Chem. Soc. Rev.* **2009**, *38*, 3316–3325.

[3] Selected reviews for metal-assisted helical structures: a) C. Piguet, G. Bernardinelli, G. Hopfgartner, *Chem. Rev.* **1997**, *97*, 2005–2062; b) M. Albrecht, *Chem. Rev.* **2001**, *101*, 3457–3497; c) J. R. Nitschke, *Acc. Chem. Res.* **2007**, *40*, 103–112; d) R. W. Saalfrank, H. Maid, A. Scheurer, *Angew. Chem.* **2008**, *120*, 8924–8956; *Angew. Chem. Int. Ed.* **2008**, *47*, 8794–8824.

[4] Selected books for anion binding: a) *Supramolecular Chemistry of Anions* (Eds.: A. Bianchi, K. Bowman-James, E. García-España), Wiley-VCH, New York, **1997**; b) *Fundamentals and Applications of Anion Separations* (Eds.: R. P. Singh, B. A. Moyer), Kluwer Academic/Plenum Publishers, New York, **2004**; c) *Anion Sensing, Topics in Current Chemistry, Vol. 255* (Ed. I. Stibor), Springer, Berlin **2005**; d) J. L. Sessler, P. A. Gale, W.-S. Cho, *Anion Receptor Chemistry*, RSC, Cambridge, **2006**; e) *Structure and Bonding, Recognition of Anions, Vol. 129* (Ed.: R. Vilar), Springer, Berlin, **2008**.

[5] Selected examples of anion-assisted single helices: a) K.-J. Chang, B.-N. Kang, M.-H. Lee, K.-S. Jeong, *J. Am. Chem. Soc.* **2005**, *127*, 12214–12215; b) J.-m. Suk, S.-K. Jeong, *J. Am. Chem. Soc.* **2008**, *130*, 11868–11869; c) V. R. Naidu, M. C. Kim, J.-m. Suk, H.-J. Kim, M. Lee, E. Sim, K.-S. Jeong, *Org. Lett.* **2008**, *10*, 5373–5376; d) U.-I. Kim, J.-m. Suk, V. R. Naidu, K.-S. Jeong, *Chem. Eur. J.* **2008**, *14*, 11406–11414; e) H. Juwarker, J. M. Lendhardt, D. M. Pham, S. L. Craig, *Angew. Chem.* **2008**, *120*, 3800–3803; *Angew. Chem. Int. Ed.* **2008**, *47*, 3740–3743; f) Y. Li, A. H. Flood, *J. Am. Chem. Soc.* **2008**, *130*, 12111–12122; g) J.-i. Kim, H. Juwarker, X. Liu, M. S. Lah, K.-S. Jeong, *Chem. Commun.* **2010**, *46*, 764–766; h) Y. Hua, A. H. Flood, *J. Am. Chem. Soc.* **2010**, *132*, 12838–12840.

[6] There have been few examples of anion-assisted double helices: a) J. Sánchez-Quesada, C. Seel, P. Prados, J. de Mendoza, *J. Am. Chem. Soc.* **1996**, *118*, 277–278; b) S. J. Coles, J. G. Frey, P. A. Gale, M. B. Hursthouse, M. E. Light, K. Navakhun, G. L. Thomas, *Chem. Commun.* **2003**, 568–569; c) S. J. Brooks, L. S. Evans, P. A. Gale, M. B. Hursthouse, M. E. Light, *Chem. Commun.* **2005**, 734–736.

[7] a) H. Maeda in *Handbook of Porphyrin Science, Vol. 8* (Eds.: K. M. Kadish, K. M. Smith, R. Guilard), World Scientific, New Jersey, **2010**, Chapter 38; b) H. Maeda in *Anion Complexation in Supramolecular Chemistry, Topics in Heterocyclic Chemistry, Vol. 24* (Eds.: P. A. Gale, W. Dehaen), Springer, Berlin, **2010**, pp. 103–144; c) H. Maeda in *Supramolecular Soft Matter: Applications in Materials and Organic Electronics* (Ed.: T. Nakanishi), Wiley, submitted; d) H. Maeda, Y. Haketa, *Pure Appl. Chem.*, DOI: 10.1351/PAC-CON-10-09-34.

[8] a) H. Maeda, Y. Kusunose, *Chem. Eur. J.* **2005**, *11*, 5661–5666; b) H. Maeda, Y. Haketa, T. Nakanishi, *J. Am. Chem. Soc.* **2007**, *129*, 13661–13674; c) H. Maeda, Y. Haketa, *Org. Biomol. Chem.* **2008**, *6*, 3091–3095; d) H. Maeda, Y. Ito, Y. Haketa, N. Eifuku, E. Lee, M. Lee, T. Hashishin, K. Kaneko, *Chem. Eur. J.* **2009**, *15*, 3706–3719; e) H. Maeda, Y. Bando, Y. Haketa, Y. Honsho, S. Seki, H. Nakajima, N. Tohnai, *Chem. Eur. J.* **2010**, *16*, 10994–11002; f) Y. Haketa, S. Sasaki, N. Ohta, H. Masunaga, H. Ogawa, N. Mizuro, F. Araoka, H. Takezoe, H. Maeda, *Angew. Chem.* **2011**, DOI: 10.1002/ange.201006356; *Angew. Chem. Int. Ed.* **2011**, DOI: 10.1002/anie.201006356; g) Y. Haketa, S. Sakamoto, T. Nakanishi, H. Maeda, unpublished results.

[9] Details for **2a**·Cl^- and **3a**·Cl^-_2 are summarized in the Supporting Information.

[10] Bridging aryl units are essential for controlling anion-binding modes, as suggested by the observation that thiophene-bridged dimer exhibits [1+1]- and [1+2]-type complexes in the presence of an excess amount of Cl^- in CD_2Cl_2.

[11] *Gaussian 03* (Revision C.01), M. J. Frisch, G. W. Trucks, H. B. Schlegel, G. E. Scuseria, M. A. Robb, J. R. Cheeseman, J. A. Montgomery, Jr., T. Vreven, K. N. Kudin, J. C. Burant, J. M. Millam, S. S. Iyengar, J. Tomasi, V. Barone, B. Mennucci, M. Cossi, G. Scalmani, N. Rega, G. A. Petersson, H. Nakatsuji, M. Hada, M. Ehara, K. Toyota, R. Fukuda, J. Hasegawa, M. Ishida, T. Nakajima, Y. Honda, O. Kitao, H. Nakai, M. Klene, X. Li, J. E. Knox, H. P. Hratchian, J. B. Cross, C. Adamo, J. Jaramillo, R. Gomperts, R. E. Stratmann, O. Yazyev, A. J. Austin, R. Cammi, C. Pomelli, J. W. Ochterski, P. Y. Ayala, K. Morokuma, G. A. Voth, P. Salvador, J. J. Dannenberg, V. G. Zakrzewski, S. Dapprich, A. D. Daniels, M. C. Strain, O. Farkas, D. K. Malick, A. D. Rabuck, K. Raghavachari, J. B. Foresman, J. V. Ortiz, Q. Cui, A. G. Baboul, S. Clifford, J. Cioslowski, B. B. Stefanov, G. Liu, A. Liashenko, P. Piskorz, I. Komaromi, R. L. Martin, D. J. Fox, T. Keith, M. A. Al-Laham, C. Y. Peng, A. Nanayakkara, M. Challacombe, P. M. W. Gill, B. Johnson, W. Chen, M. W. Wong, C. Gonzalez, J. A. Pople, Gaussian, Inc., Wallingford CT, **2004**.

[12] DOSY of **2b**, **2b**·Cl^-, and **3a**·Cl^-_2 in CD_2Cl_2 show no distinct diffusion coefficients (D) as $-\log D$ of 9.37, 9.48, and 9.48, respectively, thereby suggesting no significant differences in their sizes even though the oligomers form folded structures as TBA complexes.

[13] Cyclic double helix that contains two anions: D. Meshcheryakov, V. Böhmer, M. Bolte, V. Hubscher-Bruder, F. Arnaud-Neu, H. Herschbach, A. van Dorsselaer, I. Thondorf, W. Mögelin, *Angew. Chem.* **2006**, *118*, 1679–1682; *Angew. Chem. Int. Ed.* **2006**, *45*, 1648–1652.

[14] The K_1 and K_2 values of **3a** were estimated by *SPANA v. 2.03: Spectral Analyses Program* (developed by Prof. Yasuhisa Kuroda, Kyoto Institute of Technology).

[15] D. D. Hennings, T. Iwama, V. H. Rawal, *Org. Lett.* **1999**, *1*, 1205–1208.

[16] Similar anion-binding sandwichlike dimers in solution state have already been reported: a) S. Kubik, R. Goddard, R. Kirchner, D. Nolting, J. Seidel, *Angew. Chem.* **2001**, *113*, 2722–2725; *Angew. Chem. Int. Ed.* **2001**, *40*, 2648–2651; b) K. H. Choi, A. D. Hamilton, *J. Am. Chem. Soc.* **2001**, *123*, 2456–2457; c) K. H. Choi, A. D. Hamilton, *J. Am. Chem. Soc.* **2003**, *125*, 10241–10249; d) Z. Rodriguez-Docampo, S. I. Pascu, S. Kubik, S. Otto, *J. Am. Chem. Soc.* **2006**, *128*, 11206–11210; e) Y. Li, M. Pink, J. A. Karty, A. H. Flood, *J. Am. Chem. Soc.* **2008**, *130*, 17293–17295.

[17] Recent examples of macrocycles that exhibit high anion-binding constants, which were estimated in different solvents and cannot be compared with that of **4a**: a) K-J. Chang, D. Moon, M. S. Lah, K-S. Jeong, *Angew. Chem.* **2005**, *117*, 8140–8143; *Angew. Chem. Int. Ed.* **2005**, *44*, 7926–7929; b) J. L. Sessler, D. An, W-S. Cho, V. Lynch, M. Marquez, *Chem. Commun.* **2005**, 540–542.

[18] CrystalStructure (Ver. 3.8), Single Crystal Structure Analysis Software, Rigaku/MSC and Rigaku Corporation, The Woodlands, **2006**.

[19] A. L. Spek, *PLATON, A Multipurpose Crystallographic Tool*, Utrecht University, Utrecht, **2005**.

[20] P. van der Sluis, A. L. Spek, *Acta Crystallogr. Sect. A* **1990**, *46*, 194–201.

Received: September 24, 2010
Published online: December 16, 2010

